J Fluoresc (2014) 24:827–834
DOI 10.1007/s10895-014-1357-4

ORIGINAL PAPER

Sensitive and Selective PET-Based π-expanded Phenanthrimidazole Luminophore for Zn^{2+} Ion

J. Jayabharathi · P. Ramanathan · V. Thanikachalam · A. Arunpandiyan

Received: 12 November 2013 / Accepted: 27 January 2014 / Published online: 18 February 2014

Abstract The novel photoinduced electron transfer (PET) chemosensor, 1-(1-(4-methoxyphenyl)-1H-phenanthro[9,10-d]imidazol-2-yl)naphthalen-2-ol [MPPN] and its zinc complex were synthesised and characterized by electronic spectral and Frontier molecular orbital energy analysis. MPPN becomes efficient fluorescent chemosensor upon binding with metal ions and shows a strong preference toward Zn^{2+} ion. Density Functional theory (DFT) calculations reveal that luminescence of free MPPN originates from its orbital structure in which two π-orbitals (HOMO and HOMO-1) of the imidazole ring are situated between two π-orbitals (HOMO-2 and LUMO) of the naphthyl fragment. Therefore the absorption and emission processes occur between the two π- orbitals (HOMO-2 and LUMO). The two higher energy imidazole orbitals (HOMO and HOMO-1) serve as quenchers for the excited state of the molecule through nonradiative processes. Upon binding with Zn^{2+} ion, MPPN becomes a highly luminescent with λ_{emi}−421 nm. The significant enhancement of luminescence upon binding with Zn^{2+} ion is attributed to the stabilization of HOMO-2 and HOMO-1 π-orbitals of imidazole ring upon their engagement in new bonds with Zn^{2+} ion. The affinity of MPPN to zinc ion is found to be very high [K= 6×10^{6} M^{-1}] when compared with other metals ions. The nonlinear absorption coefficient γ for MPPN is 1.9×10^{-12} m/W and 3.9×10^{-11} m/W for MPPN-Zn complex.

Keywords MPPN · PET · Chemosensor · Nonlinear optical properties · DFT method

J. Jayabharathi (✉) · P. Ramanathan · V. Thanikachalam · A. Arunpandiyan
Department of Chemistry, Annamalai University, Annamalainagar 608 002, Tamilnadu, India
e-mail: jtchalam2005@yahoo.co.in

Introduction

2The development of fluorescent indicators are sensitive to biologically relevant substrates such as zinc [1–6], magnesium [7–9] and alkali metal cations [10–15], anions such as halides [16–26] and carboxylates [27–31] is of enormous interest to biology-related research and also for medical diagnostics. Among the several detection mechanisms, photoinduced energy transfer (PET) appears to be the most elegant, sensitive and effective way to identify the presence of protons [32–34], metal ions [35], anions [16–26, 36–40] and even uncharged molecules [41–49]. The PET chemosensor consists of a luminescent species which is attached to a recognition group [50–54]. In the unbound molecule, the binding group efficiently quenches the excited state of the luminescent part. This is normally achieved through electron energy transfer processes that takes place between the lone pair electrons of the recognition group and the relevant orbitals of the luminophore that are involved in the optical absorption and emission processes. Therefore, upon binding, the lone pair of the recognition group becomes engaged in the newly formed bond and can no longer serve as an efficient quencher for the luminophore. Thus, these kind of systems regain their luminescence upon binding a guest and are therefore capable of signaling its capture. In this article we report the synthesis, quantum chemical studies and excited state intramolecular proton transfer (ESIPT) analysis of the newly synthesized (1-(4-methoxyphenyl)-1H-phenanthro[9,10-d]imidazol-2-yl)naphthalen-2-ol [MPPN]. We have also addressed a new phenanthrimidazole (MPPN) based PET chemosensor for zinc ion. In continuation of our research [55–63] toward the molecular hyperpolarizability we found that a phenanthrimidazole derivative makes the zinc complex as the potential NLO material.

Experimental

Spectral Measurements

The infrared spectra were recorded with an Avatar 330-Thermo Nicolet FT-IR spectrometer. The ^{1}H and proton decoupled ^{13}C NMR spectra of MPPN and its zinc complex in dimethyl sulphoxide (DMSO) were recorded at room temperature using a Bruker 400 MHz NMR spectrometer operating at 400 and 100 MHz, respectively. The mass spectra were obtained using a Thermo Fischer LC-Mass spectrometer in fast atom bombardment (FAB) mode. The UV–vis absorption and fluorescence spectra were recorded in both polar and nonpolar solvents with PerkinElmer Lambda 35 spectrophotometer and PerkinElmer LS55 spectrofluorimeter, respectively. Required volume of aqueous solution of metal ions of desired concentration was added to the solution of 1×10^{-5} M of MPPN in dioxane, sonicated and electronic spectrum were recorded.

Computational Details

The quantum chemical calculations were performed using the Gaussian-03 [64] package. Computation of optimization and HOMO and LUMO frontier orbitals were performed using density functional theory (DFT) method.

Facile and Rapid Synthesis of 1-(1-(4-methoxyphenyl) -1H-phenanthro[9,10-d]imidazol-2-yl)naphthalen-2-ol [MPPN] by InF_3

A mixture of 2-hydroxynaphthaldehyde (1 mmol), phenanthroquinone (1 mmol), 4-methoxyaniline (1 mmol), ammonium acetate (1 mmol) and InF_3 (1 mol %) was stirred at 80 °C. The progress of the reaction was monitored by TLC [65]. The reaction, the mixture was cooled and filtered. The product was purified by column chromatography using benzene: ethyl acetate (9:1) as the eluent. M.p. 231ºC. Anal. calcd. for $C_{32}H_{22}N_2O_2$: C, 82.38; H, 4.75; N, 6.00 . Found: C, 82.08; H, 4.70; N, 5.92. ^{1}H NMR (400 MHz, DMSO): δ 3.72 (s, 3H), 8.96 (d, *J*=8.4Hz, 1H), 8.91 (d, *J*=8.4Hz, 1H), 8.66 (d, *J*=7.6Hz, 1H), 7.89 (d, *J*=8.0Hz, 1H), 7.76 (d, *J*= 7.2Hz, 1H), 7.57 (d, *J*=7.6Hz, 1H), 7.38 (t, 1H), 7.20 (d, *J*= 8.0Hz, 1H), 7.96 (t, 2H), 7.69 (t, 2H),7.55–7.42 (m, 5H), 6.94 (d, *J*=8.4Hz, 2H), 12.93 (s, 1H). ^{13}C NMR (100 MHz, DMSO): δ 55.28, 114.62, 120.27, 121.98, 122.59, 123.66, 124.42, 124.67, 125.19, 125.60, 125.78, 126.20, 126.69, 126.82, 126.86, 127.24, 127.42, 127.64, 128.04, 128.09, 128.29, 128.41, 129.50, 129.52, 129.72, 129.95, 132.35, 132.76, 136.28, 150.47, 159.47. MS: m/z. 466 [M^{+}]. IR (cm^{-1}): 1625, 1125, 2210.

Synthesis of MPPN- Zn

The ligand MPPN (1 mmol) and $Zn(CH_3COO)_2{\cdot}4H_2O$ (0.5 mmol) were dissolved in ethanol (20 mL) in the molar ratio of 2:1. The solution stirred for 3 days at room temperature. The formed crystals were filtered. Anal. calcd. for $C_{32}H_{21}N_2O_2Zn$: C, 72.39; H, 3.99; N, 5.28. Found: C, 72.08; H, 3.81; N, 5.03. ^{1}H NMR (400 MHz, DMSO): δ 3.01 (s, 3H), 8.90 (d, 1H), 8.53 (d, 1H), 7.78 (s, 1H), 7.51 (d, 2H), 7.25 (s, 2H), 7.90 (t, 2H), 7.51–7.22 (m, 7H). ^{13}C NMR (100 MHz, DMSO): δ 54.91, 112.62, 122.05, 124.01, 125.98, 126.43, 126.89, 127.30, 128.21, 128.63, 129.49, 129.92, 132.82, 136.92, 150.01, 153.92. MS: m/z. 529.09 [M^{+}]. IR (cm^{-1}): 937.12 (Zn–O), 465.68 (Zn–N).

Results and Discussion

ESIPT Process

Absorption and emission spectra of MPPN have been recorded (Fig. 1). The fluorescence spectra in dioxane display a dual emission, one emission band at shorter wavelength 310 nm and another peak at longer wavelength 408 nm. The emission peak at shorter wavelength (310 nm) is assigned to rotamer **I** (exist with intramolecular hydrogen bonded isomeric form) and that at the longer wavelength (408 nm) is assigned to rotamer **II**. Excitation of isomer **I** lead to the formation of keto-isomer **II** due to ESIPT (Fig. 2a). Stokes shift is important for a fluorescent sensor. The higher stokes shift supplies very low background signal and allows the usage of the material in construction of a fluorescence sensor [66].

However in hydroxylic solvent, a short wavelength emission band appears due to the presence of intermolecular hydrogen bonding with hydroxylic solvent leading to the stabilization of solvated isomer **III** in which ESIPT is impossible. The parent compound 1-(4-methoxyphenyl)-2-(naphthalen-1-

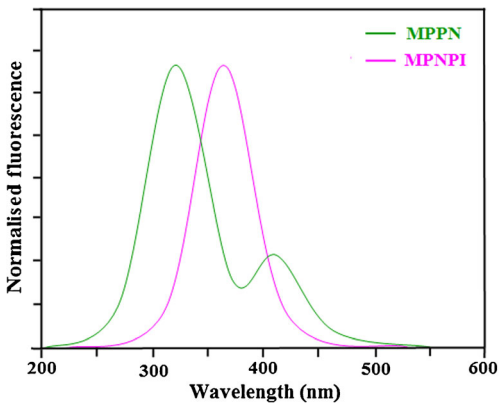

Fig. 1 Room temperature emission spectra of MPPN and its parent MPNPI

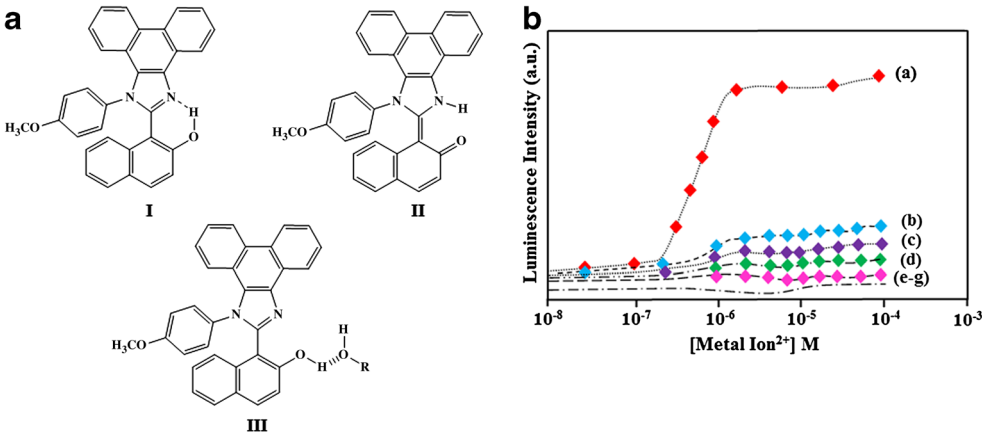

Fig. 2 **a** Various isomeric forms of MPPN; **b** Relative emission intensities of a solution of 1×10^{-5} M of MPPN in dioxane in the presence of different metal ions: (*a*) $Zn(NO_3)_2$, (*b*) $Cd(NO_3)_2$, (*c*) $Mg(NO_3)_2$, (*d*) $Cu(NO_3)_2$, (*e*) $LiNO_3$, (*f*) $NaNO_3$ and (*g*) KNO_3 with different concentrations of 0 M, 9.85×10^{-8} M, 4.88×10^{-7} M, 8.90×10^{-7} M, 3.00×10^{-6} M, 4.86×10^{-6} M, 7.45×10^{-6} M, 9.42×10^{-6} M

yl)-1H-phenanthro[9,10-d]imidazole (MPNPI) exhibits emission peak only at 368 nm, absence of additional peak at longer wavelength confirms the absence of intramolecular hydrogen bond in parent compound. It is evident that intramolecular hydrogen bonding is the driving force for ESIPT and the dual fluorescence behaviour of MPPN [67–69]. The existence of intramolecular hydrogen bond is confirmed by the presence of singlet at 12.93 ppm in the ^{1}H NMR spectra which is found as the driving force for ESIPT process.

Relative Stability of Different Conformers

A simplified schematic photoinduced proton transfer process in MPPN is presented in Fig. 2a in which enol-form represents

Table 1 Selected optimized geometry parameters for the enol and keto-forms and Zn-Complex

Geometry parameters	MPPN		Geometry parameters	MPPN - Zn
	Enol-form	Keto-form		
Bond length (Å)			Bond length (Å)	
O_{34}-H_{53}	1.01	2.09	C_{10}-N_{17}	1.44
N_{17}-C_{16}	1.35	1.46	C_{16}-N_{17}	1.28
O_{34}-C_{26}	1.43	1.27	N_{15}-C_{16}	1.48
			C_7-N_{15}	1.50
N_{17}-H_{53}	2.49	1.01	C_{16}-C_{24}	1.65
N_{17}-C_{10}	1.47	1.51	C_{24}-C_{26}	1.61
C_{16}-C_{24}	1.54	1.36	C_{26}–O_{34}	1.51
C_{24}-C_{26}	1.36	1.51	O_{34}-Zn_{54}	1.78
N_{17}-C_{10}	1.47	1.45	N_{17}-Zn_{54}	1.80
N_{15}-C_{18}	1.47	1.46	N_{15}-C_{18}	1.47
Bond angle (°)			Bond angle (°)	
H_{53}-O_{34}-C_{26}	109.8	–	C_{10}-N_{17}-Zn_{54}	143.7
N_{17}-H_{54}-O_{34}	81.2	–	C_{26}-O_{34}-Zn_{54}	93.4
C_{24}-C_{26}- O_{34}	119.7	125.4	N_{17}-C_{16}-C_{24}	120.8
N_{17}-C_{16}-C_{24}	124.6	118.9	N_{15}-C_{16}-C_{24}	131.3
Dihedral angle (°)			Dihedral angle (°)	
N_{15}-C_{16}-C_{24}-C_{25}	3.0	18.0	C_{16}-C_{17}-C_{16}-C_{24}	167.7
N_{17}-C_{16}-C_{24}-C_{26}	3.6	–	C_{10}-C_{17}-Zn_{54}-O_{34}	139
N_{17}-C_{16}-C_{26}-O_{34}	0.4	48.9	C_{24}-C_{26}-O_{34}-Zn_{54}	151
H_{53}-C_{34}-C_{26}-C_{24}	69.2	–	N_{15}-C_{16}-C_{17}-Zn_{54}	171
H_{58}-N_{57}-C_{16}-C_{23}	–	87.9	–	–

Table 2 Relative energy (ΔE kcal/mol), dipole moment (μ, D), Mulliken charges and HOMO-LUMO energies (eV) of MPPN

Comd.	ΔE	μ	N_{17}	O_{33}	HOMO	LUMO	HOMO-1	LUMO+1
Enol-form	0.00	3.1	−0.185	−0.285	−8.46	−5.06	−9.03	−4.42
Keto-form	23.1	5.9	−0.125	−0.318	−7.31	−2.76	−8.50	−0.68

the ground-state geometry of the enolic conformer and keto-form is the proton transferred geometry of the molecule. Few important optimized geometry parameters [DFT/B3LYP/6-31G(d,p)] relevant to ESIPT are summarized in Table 1. The N_{17}–C_{10}, N_{17}–C_{16}, O_{34}–H_{53} and C_{24}–C_{26} bond lengths are enlarged on going from enol to keto isomer whereas O_{34}–C_{26}, N_{17}–H_{53} and C_{16}–C_{24} distances are shortened. Such modulation in the bond distances from enol to keto isomer rationalized by the reduced double bond character of the bonds in the former cases and increase of the same in the latter cases. As far as the angular changes are concerned, the angle <H_{53}-O_{34}-C_{26} is considerably shortened while the angle <N_{17}-H_{54}-O_{34} undergoes enlargement on passing from enol to keto-form. The variation of the optimized geometry parameters during enol → keto transition is in accordance with the geometric reorganization required in course of an ESIPT process. Moreover the intramolecular hydrogen bond distance (H_{53}…N_{17}) in the enol-form is predicted to be 2.49 Å. This is longer than usual hydrogen bond distances involving six-member hydrogen bonding ring type [70–73].

The data compiled in Table 2 throw light on the relative stabilities of the enol and keto forms in the ground-state. Calculation predicts the enol-form is the lowest energy conformer in the ground-state, while the keto-form is appreciably unstable, 23.07 kcal/mol higher with respect to the enol-form. Such high degree of instability of the keto-form in the ground-state is a strong corroboration to the non-viability of ground-state intramolecular proton transfer (GSIPT) reaction. The ground-state dipole moment of keto-form (5.9 D) is remarkably higher than that of enol-form (3.1 D). Such enlargement of dipole moment for keto-geometry provided us the impetus to extend the calculations further so as to be able to delineate the influence of solvent reaction field on the relative stabilities of various conformers and optimized geometry parameters.

Electronic Spectral Analysis

The absorption spectra of MPPN show a superposition of the bands corresponding to the donor and acceptor subunits which seem to be only slightly perturbed by their interactions. The three absorption bands at 358, 307 and 288 nm are assigned to $^1(\pi\text{-}\pi^*)$ transition correspond in Platt's notation to ^1L_b , ^1L_a and ^1B_a excited states. The low and high energy transitions, $^1L_b \leftarrow S_0$, $^1L_a \leftarrow S_0$ and $^1B_a \leftarrow S_0$, respectively, with a relatively high probability can be clearly observed in the absorption spectra [74, 75]. Detailed inspection of low-energy absorption region of the phenanthrimidazole derivative containing naphthyl as an electron acceptor clearly indicates the presence of additional charge transfer singlet states. A long wave shoulder attributed to $^1CT \leftarrow S_0$ transition is also observed. The magnitude of the shifts suggests that the ground state of the molecule is polar.

The absorption around 399 and 408 nm can be assigned to metal → ligand charge transfer (MLCT) and ligand → ligand charge transfer (LLCT) for Zn-MPPN. The high energy transitions 258 and 281 nm are from intra-ligand π-π* transitions. The HOMOs have about 2.5 % contribution for MPPN – Zn of central metal ion, while the LUMO and LUMO+1 is nearly localized on ligand. Therefore, the lowest energy absorption is assigned as the LLCT and mixed with MLCT. Figure 2b depicts the absorption of MPPN are found to be very sensitive to the presence of even submicromolar traces of zinc ion.

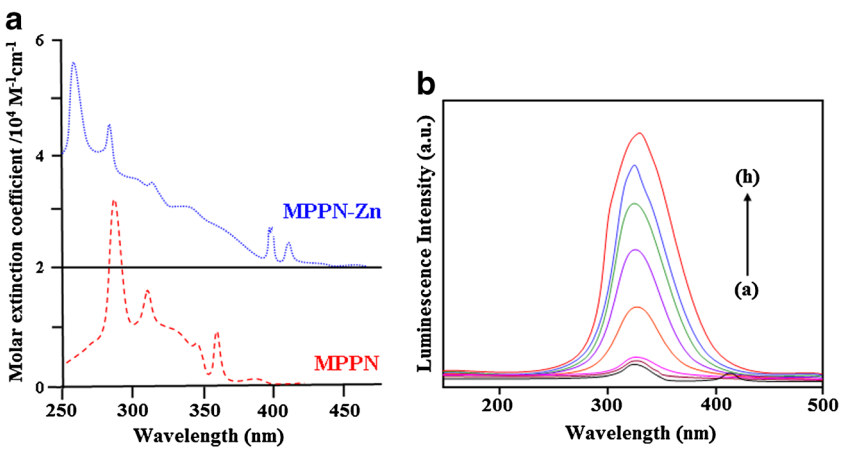

Fig. 3 **a** Absorption spectra of MPPN and MPPN-Zn; **b** Emission spectra of a solution of 1×10^{-5} M MPPN in the presence of different concentrations of Zn^{2+} $(NO_3)_2$, (*a*) 0 M, (*b*) 9.85×10^{-8} M, (*c*) 4.88×10^{-7} M, (*d*) 8.90×10^{-7} M, (*e*) 3.00×10^{-6} M, (*f*) 4.86×10^{-6} M, (*g*) 7.45×10^{-6} M, (*h*) 9.42×10^{-6} M

Table 3 Binding constant (***K***) between MPPN and different metal ions

Ion	K (M^{-1})
Zn^{2+}	6×10^6
Cd^{2+}	2×10^4
Mg^{2+}	6×10^2
Cu^{2+}	4×10^3
Li^+	Less sensitive
Na^+	Less sensitive
K^+	Less sensitive

Binding constant K was calculated according to the Benesi-Hildebrand equation, $1/(A-AO)=1/\{K(A_{max}-AO)\ [Zn^{2+}]_n\}+1/[A_{max}-A_O]$, here A_o is the absorbance of receptor in the absence of Zn^{2+}, A is the absorbance recorded in the presence of Zn^{2+}, A_{max} is absorbance in presence of added $[Zn^{2+}]_{max}$ and K is the binding constant (M^{-1}). The binding constant (K) could be determined from the slope of the straight line of the plot of $1/(A-A_o)$ against $1/[\ Zn^{2+}]$, confirming 1:1 binding between MPPN and Zn^{2+} with binding constant, $K=6\times10^6$ and slope=1.05 ($r^2=0.99$) [76, 77].

Addition of even trace amount of zinc ion results increase of the luminescence of MPPN (Fig. 3a). The affinity of chromophore toward other metal ions, such as Cd^{2+}, Cu^{2+} and Mg^{2+} is significantly lower than that for Zn^{2+} as can be seen in Fig. 3b. The apparent binding constants (K) have been obtained from the fluorescence data using the following equation, $1/(F-F_0') = 1/(F-F_0) + 1/K\ (F-F_0)$ [MPPN], where K is the binding constant, F_0 is the fluorescence intensity of the bare imidazole derivative, F is the fluorescence intensity of the complex. A good linear relationship was obtained by the plot of $1/(F-F_0)$ and the reciprocal concentration with the binding constant $K=6.2\times10^6$ for MPPN-Zn which is similar with that calculated from absorbance data. Table 3 depicts the different binding constants calculated from the metal induced gain in luminescence. The fluorescence intensity of MPPN was found to be practically independent of the presence of Li^+, Na^+ and K^+ ions and the weaker effect of these ions is indicative of the reduced affinity of MPPN toward those ions.

The enhancement in fluorescence intensity of MPPN on interaction with Zn^{2+} may be explained on the basis of the thermodynamically favourable photo induced electron transfer (PET) mechanism [78] between MPPN and Zn^{2+}. The Zn^{2+} ion bind to MPPN via lone pair of electron of the azomethine nitrogen atom and recognition group of the phenanthrimidazole moiety. The PET process occurs due to the transfer of electron density, originating at the lone pair of electrons on nitrogen atom of the imidazole moiety, to the LUMO of the fluorophore. Binding of Zn^{2+} to MPPN through the nitrogen atom lone pair will obviously hinder the PET process leading to fluorescence intensity enhancement of MPPN on interaction with Zn^{2+} ion (Scheme 1). The cyclic voltammogram of MPPN and MPPN- Zn was recorded in 1:1 (*v*/*v*) DMSO: H_2O. An irreversible cyclic voltammogram was obtained at +0.298 V for MPPN. The effect of Zn^{2+} on the voltammogram was investigated by adding different concentration of Zn^{2+} in the electrolytic medium. On interaction with Zn^{2+} the irreversible cyclic voltammogram observed for MPPN became quasi reversible with reduction peak at + 0.129 V and oxidation peak at +0.452 V (Fig. 4).

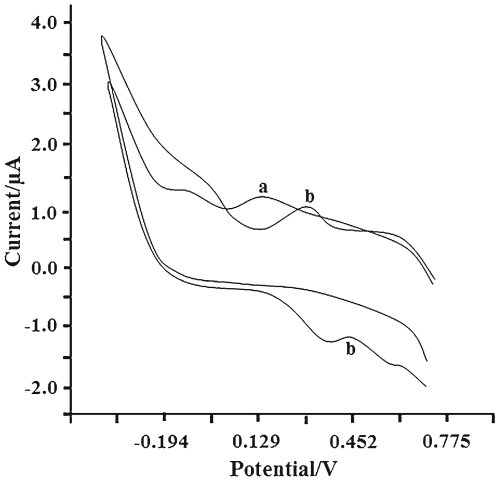

Fig. 4 Cyclic voltammetric response of 1 mM solution of MPPN in 1:1 (*v*/*v*) DMSO:H_2O

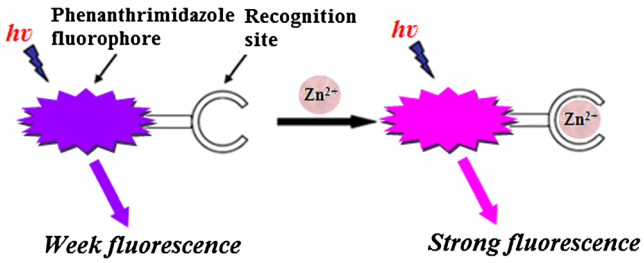

Scheme 1 Metal ion sensing by fluorescent photoinduced electron transfer (PET) indicators

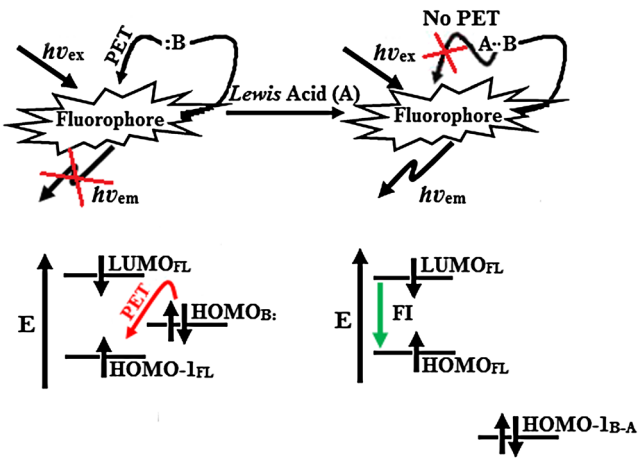

Scheme 2 Energy diagram of PET based sensing

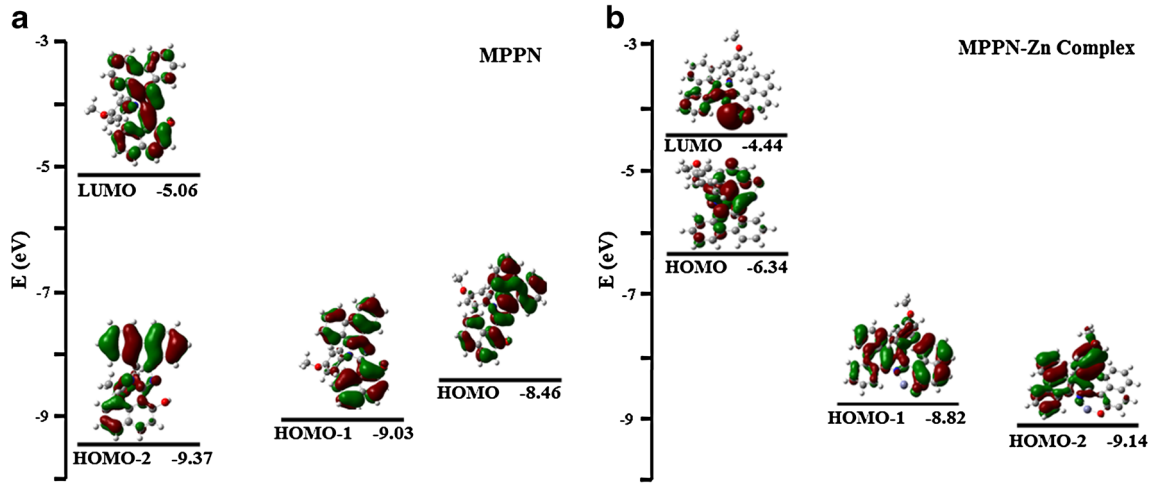

Fig. 5 **a** Orbital energy diagram for MPPN (Gaussian 03software package, B3LYP/ 6-31G (d,p)); **b** Orbital energy diagram for MPPN-Zn (Gaussian 03 software package, B3LYP/6-31G (d,p))

Frontier Molecular Orbital Energy Analysis

Orbital energy level diagram for the free host MPPN and its zinc complex MPPN- Zn by DFT analysis shows that the PET of MPPN is due to the presence of lone pair of electrons on azomethine nitrogen which behave as a quencher and also binding site for metal ion (Scheme 2). The energies of the LUMO, HOMO, HOMO-1, HOMO-2 and any other relevant orbital of the energy minimized systems were extracted from the calculations and presented in Fig. 5a & b for the free host and its zinc complex respectively. Luminescence of free MPPN originates from its orbital structure in which two π-orbitals (HOMO and HOMO-1) of the imidazole ring are situated between two π - orbitals (HOMO-2 and LUMO) of the naphthyl fragment. The two π-orbitals of the imidazole ring are located between the two π-orbitals that participate in photoexcitation and photoluminescence which is indicative of a PET system. In contrast, the lone pair of nitrogen atom of imidazole ring is at a lower energy than HOMO-2. This explains the very low luminescence efficiency found for the free host. In the Zinc complex, both the HOMO and LUMO π-orbitals participate in the photoexcitation and photoluminescence processes. The π-orbitals of imidazole ring located at HOMO-1 and HOMO-2 which are low in energy than HOMO so that the luminescence enhanced.

Nonlinear Absorption Components

The nonlinear absorption components have been evaluated by Z-scan method indicate that the absorption increases as the incident light irradiance rises. The normalized transmittance is about 76 % for MPPN and 70 % for complex and the nonlinear absorption coefficient γ for MPPN is 1.9×10^{-12} m/W and 3.9×10^{-11} m/W for MPPN-Zn complex. It is obvious that the complex exhibit very strong NLO absorption [79, 80]. According to the frontier molecular orbital theory, orbitals of HOMO–LUMO and related orbitals are important to the electronic properties of the complex. HOMO is usually as the donor and the LUMO is an acceptor. These frontier orbitals are primarily composed of d orbitals of metal ion in the zinc complex and π - orbitals of oxygen and nitrogen atoms. It is well known that stronger delocalization of electrons make the system as potential NLO candidate. Thus, complex should have better NLO properties than MPPN. The NLO properties were affected by the energy gap, smaller energy gap make the system as better NLO material. Figure 5a & b show that MPPN tend to have largest energy gap compared with complex which has the minimum. So that the zinc complex exhibit strong NLO properties than the MPPN. This is consistent with the experimental NLO results in this study.

Conclusion

A new phenanthrimidazole-based PET system, 1-(1-(4-methoxyphenyl)-1H -phenanthro[9,10-d]imidazol-2-yl)naphthalen-2-ol (MPPN), was synthesised and characterized by its affinity to different metal ions. This new material shows potential affinity toward Zn^{2+} ion and its zinc complex is found to be more fluorescent than free host. To rationalize the experimental results, DFT calculations were made, in which the two π-orbitals of the imidazole ring of free luminophore serve as quencher for the excited state. In the complex, the π-orbitals of the imidazole ring are stabilized and can no longer serve as quencher to the excited state of the luminophore. Therefore, the luminescence of MPPN is enhanced upon binding of Zn^{2+} ion. MPPN- Zn complex shows strong NLO absorptive properties when compared with MPPN which shows slightly weaker and the nonlinear absorption coefficient γ for MPPN is 1.9×10^{-12} m/W and 3.9×10^{-11} m/W for MPPN-Zn complex. Based on Frontier

molecular orbital calculations, MPPN has largest energy gap and complex has the minimum and exhibit better NLO property.

Acknowledgments One of the authors Prof. J. Jayabharathi is thankful to DST [No. SR/S1/IC-73/2010], DRDO (NRB-213/MAT/10-11), UGC (F. No. 36-21/2008 (SR)) and CSIR (NO 3732/NS-EMRII) for providing funds to this research study.

References

1. Sankaran NB, Banthia S, Das S, Samanta A (2002) Fluorescence signaling of transition metal ions: a new approach. New J Chem 26: 1529–1531
2. Cordier D, Coulet PR (1994) Metal-ion complexation by a new urea macrocyclophane. J Chem Soc Perkin Trans 2:891
3. Krauss R, Weinig H-G, Seydack M, Bendig J, Koert U (2000) Molecular signal transduction via a perhydroanthracene transducer by conformational transmission. Angew Chem Int Ed 39:1835–1837
4. Pina F, Bernardo MA, Garcia-Espana E (2000) Fluorescent chemosensors containing polyamine receptors. Eur J Inorg Chem 10:2143–2157
5. Ressalan S, Iyer CSP (2005) Absorption and fluorescence spectroscopy of 3-hydroxy-3-phenyl-1-*o*-carboxy phenyltriazene and its copper (II), nickel (II) and zinc (II) complexes: a novel fluorescence sensor. J Lumin 111:121–129
6. de Silva AP, Gunaratne HQN, Gunnlaugsson T, Huxley AJM, McCoy CP, Rademacher JT, Rice TE (1997) Signaling recognition events with fluorescent sensors and switches. Chem Rev 97:1515–1566
7. Liu Y, Duan Z-Y, Zhang H-Y, Jiang X-L, Han J-R (2005) Selective binding and inverse fluorescent behavior of magnesium ion by podand possessing plural imidazo[4,5-*f*]-1,10-phenanthroline groups and its Ru(II) complex. J Org Chem 70:1450–1455
8. Pond SJK, Tsutsumi O, Rumi M, Kwon O, Zojer E, Bredas J-L, Marder SR, Perry JW (2004) Metal-ion sensing fluorophores with large two-photon absorption cross sections: aza-crown ether substituted donor-acceptor-donor distyryl benzenes. J Am Chem Soc 126:9291–9306
9. Pearson AJ, Xiao WJ (2003) Fluorescence and NMR binding studies of *N*-Aryl-*N*'-(9-methylanthryl)diaza-18-crown-6 derivatives. J Org Chem 68:5369–5376
10. Bu J-H, Zheng Q-Y, Chen C-F, Huang Z-T (2004) New fluorescence-quenching process through resumption of PET process induced by complexation of alkali metal ion. Org Lett 6:3301–3303
11. Nakahara Y, Kida T, Nakatsuji Y, Akashi M (2005) Fluorometric sensing of alkali metal and alkaline earth metal cations by novel photosensitive monoazacryptand derivatives in aqueous micellar solutions. Org Biomol Chem 3:1787–1794
12. Tuncer H, Erk C (2005) Association constants of dibenzo[3*n* + 2]crown-*n* ethers using steady-state fluorescence spectroscopy. Talanta 65:819–823
13. Liu Y, Duan Z-Y, Chen Y, Han J-R, Lu C (2004) Cooperative self-assembly and molecular binding behavior of cyclodextrin–crown ether conjugates mediated by alkali metal ions. Org Biomol Chem 2:2359–2364
14. McSkimming G, Tucker JHR, Bouas-Laurent H, Desvergne J-P, Coles SJ, Hursthouse MB, Light ME (2002) Photoinduced formation of a cryptand from a coronand: an unexpected switch in cation binding affinity. Chem Eur J 8:3331–3342
15. Sankaran NB, Nishizawa S, Watanabe M, Uchida T, Teramae N (2005) Designing ratiometric fluorescent sensors for alkali metal ions from simple PET sensors by controlling spacer length. J Mater Chem 15:2755–2761
16. Salman H, Abraham Y, Tal S, Meltzman S, Kapon M, Tessler N, Speiser S, Eichen Y (2005) 1,3-Di(2-pyrrolyl)azulene: an efficient luminescent probe for fluoride. Eur J Org Chem 11:2207–2212
17. Kang J, Kim J (2005) Bromide selective fluorescent anion receptor with glycoluril molecular scaffold. Tetrahedron Lett 46:1759–1762
18. Liu B, Tian H (2005) A highly selective chromogenic and fluorogenic chemosensor for fluoride ion. Chem Lett 34:686–687
19. Bai Y, Zhang B-G, Xu J, Duan C-Y, Dang D-B, Liu D-J, Meng Q-J (2005) Conformational switching fluorescent chemosensor for chloride anion. New J Chem 29:777–779
20. Kim H, Kang J (2005) Iodide selective fluorescent anion receptor with two methylene bridged bis-imidazolium rings on naphthalene. Tetrahedron Lett 46:5443–5445
21. Piatek P, Lynch VM, Sessler JL (2004) J Am Chem Soc 126:16073–16076
22. Ghosh T, Maiya BG, Wong MW (2004) Fluoride ion receptors based on dipyrrolyl derivatives bearing electron-withdrawing groups:? Synthesis, optical and electrochemical sensing, and computational studies. J Phys Chem A 108:11249–11259
23. Anzenbacher P, Try AC, Miyaji H, Jursikova K, Lynch VM, Marquez M, Sessler JL (2000) J Am Chem Soc 122:10268–10272
24. Xu G, Tarr MA (2004) A novel fluoride sensor based on fluorescence enhancement. Chem Commun 9:1050–1051
25. Chen C-F, Chen Q-Y (2004) A tetra-sulfonamide derivative bearing two dansyl groups designed as a new fluoride selective fluorescent chemosensor. Tetrahedron Lett 45:3957–3960
26. Black CB, Andrioletti B, Try AC, Ruiperez C, Sessler JL (1999) J Am Chem Soc 121:10438–10439
27. Gunnlaugsson T, Davis AP, O'Brien JE, Glynn M (2005) Synthesis and photophysical evaluation of charge neutral thiourea or urea based fluorescent PET sensors for bis-carboxylates and pyrophosphate. Org Biomol Chem 3:48–56
28. Wu J-L, He Y-B, Zeng Z-Y, Wei L-H, Meng L-Z, Yang T-X (2004) Synthesis of the anionic fluororeceptors based on thiourea and amide groups and recognition property for α, ω-dicarboxylate. Tetrahedron 60:4309–4314
29. Reyman D, Tapia MJ, Carcedo C, Vinas MH (2003) Photophysical properties of methyl β-carboline-3-carboxylate mediated by hydrogen-bonded complexes—a comparative study in different solvents. Biophys Chem 104:683–696
30. Gunnlaugsson T, Davis AP, O'Brien JE, Glynn M (2002) Org Lett 4: 2449–2452
31. Fabbrizzi L, Licchelli M, Parodi L, Poggi A, Taglietti A (1999) Eur J Inorg Chem 1:35–39
32. de Silva SA, Loo KC, Amorelli B, Pathirana SL, Nyakirang'ani M, Dharmasena M, Demarais S, Dorcley B, Pullay P, Salih YA (2005) J Mater Chem 15:2791–2795
33. Arunkumar E, Ajayaghosh A (2005) Chem Commun 5:599–601
34. de Silva AP, Gunaratne HQN, McCoy CP (1996) Chem Commun 21: 2399–2400
35. Grabchev I, Chovelon J-M, Qian X (2003) A polyamidoamine dendrimer with peripheral 1,8-naphthalimide groups capable of acting as a PET fluorescent sensor for metal cations. New J Chem 27:337–340
36. Gunnlaugsson T, Ali HDP, Glynn M, Kruger PE, Hussey GM, Pfeffer FM, Santos CMG, Tierney J (2005) Fluorescent photoinduced electron transfer (PET) sensors for anions: from design to potential application. J Fluoresc 15:287–299
37. Gunnlaugsson T, Davis AP, Hussey GM, Tierney J, Glynn M (2004) Org Biomol Chem 2:1856–1863
38. Gunnlaugsson T, Kruger PE, Lee TC, Parkesh R, Pfeffer FM, Hussey GM (2003) Dual responsive chemosensors for anions: the combination of fluorescent PET (Photoinduced Electron Transfer) and colorimetric chemosensors in a single molecule. Tetrahedron Lett 44: 6575–6578

39. Gunnlaugsson T, Davis AP, Glynn M (2001) Chem Commun 24: 2556–2557
40. Kubo Y, Kato M, Misawa Y, Tokita S (2004) A fluorescence-active 1, 3-bis(isothiouronium)-derived naphthalene exhibiting versatile binding modes toward oxoanions in aqueous MeCN solution: new methodology for sensing oxoanions. Tetrahedron Lett 45:3769–3773
41. Ebru Seckin Z, Volkan M (2005) Anal Chim Acta 547:104–108
42. Sahu T, Pal SK, Misra T, Ganguly T (2005) Involvements of phenyldibenzophosphole and 9-phenylcarbazole in electron transfer reactions with photoexcited 9-cyanoanthracene. J Photochem Photobiol A 171:39–50
43. Soh N, Sakawaki O, Makihara K, Odo Y, Fukaminato T, Kawai T, Irie M, Imato T (2005) Design and development of a fluorescent probe for monitoring hydrogen peroxide using photoinduced electron transfer. Bioorg Med Chem 13:1131–1139
44. Guo X, Zhang D, Zhang D, Guan Y, Zhu D (2004) Fluorescence modulation for the multimolecular communicating ensembles with light and ferric ion: photo-control of the intermolecular photoinduced electron transfer. Chem Phys Lett 398:93–97
45. Nakanishi J, Maeda M, Umezawa Y (2004) Anal Sci 20:273–278
46. Sen K, Basu S (2004) Effect of chain length on stoichiometry of complex formation between α, ω-diphenylpolyenes and N, N-dimethylaniline in excited state. Chem Phys Lett 387:61–65
47. Gabe Y, Urano Y, Kikuchi K, Kojima H, Nagano T (2004) J Am Chem Soc 126:3357–3367
48. Nakata E, Nagase T, Shinkai S, Hamachi I (2004) J Am Chem Soc 126:490–495
49. Pal SK, Bhattacharya T, Misra T, Saini RD, Ganguly T (2003) Photophysics of some disubstituted indoles and their involvements in photoinduced electron transfer reactions. J Phys Chem A 107: 10243–10249
50. Weller A (1968) Pure Appl Chem 16:115–123
51. Rehm D, Weller A (1970) Isr J Chem 8:259–271
52. de Silva AP, Eilers J, Zlokarnik G (1996) Proc Natl Acad Sci U S A 96:8336–8337
53. Leray I, Lefevre J-P, Delouis J-F, Delaire J, Valeur B (2001) Chem Eur J 7:4590–4598
54. Burdette SC, Walkup GK, Spingler B, Tsien RY, Lippard SJ (2001) J Am Chem Soc 123:7831–7841
55. Jayabharathi J, Thanikachalam V, Srinivasan N, Perumal MV, Jayamoorthy K (2011) Physicochemical studies of molecular hyperpolarizability of phenanthrimidazoles derivatives. Spectrochim Acta part A 79:137–147
56. Jayabharathi J, Thanikachalam V, Sathishkumar R, Jayamoorthy K (2013) Physico-chemical studies of fused phenanthrimidazole derivative as sensitive NLO material. Spectrochim Acta A 101:249–253
57. Jayabharathi J, Thanikachalam V, Venkatesh Perumal M (2011) Photophysical studies of fused phenanthrimidazole derivatives as versatile π-conjugated systems for potential NLO applications. Spectrochim Acta A 92:113–121
58. Jayabharathi J, Thanikachalam V, Sathishkumar R (2011) Characterization, physiochemical and computational studies of the newly synthesized novel imidazole derivative. Spectrochim Acta Part A 97:582–588
59. Jayabharathi J, Thanikachalam V, Saravanan K, Srinivasan N, Venkatesh Perumal M (2011) Physiochemical properties of organic nonlinear optical crystal from a combined experimental and theoretical study. Spectrochim Acta A 78:794–802
60. Jayabharathi J, Thanikachalam V, Vijayan N, Srinivasan N, Venkatesh Perumal M (2010) Studies on crystal growth and optical properties of organic nonlinear optical crystal—a combined experimental and theoretical study. Struct Chem Commun 1:46–52
61. Jayabharathi J, Thanikachalam V, Jayamoorthy K (2013) Optical properties of 1, 2-diaryl benzimidazole derivatives—a combined experimental and theoretical studies. Spectrochim Acta A 115:74–78
62. Jayabharathi J, Thanikachalam V, Brindha Devi K, Venkatesh Perumal M (2012) Optical properties of organic nonlinear optical crystal—a combined experimental and theoretical study. Spectrochim Acta A 86:69–75
63. Subramanian N, Sundaraganesan N, Jayabharathi J (2010) Molecular structure, spectroscopic (FT-IR, FT-Raman, NMR, UV) studies and first-order molecular hyperpolarizabilities of 1,2-bis(3-methoxy-4-hydroxybenzylidene)hydrazine by density functional method. Spectrochim Acta A 76:259–269
64. Frisch MJ, Trucks GW, Schlegel HB, Scuseria GE, Robb MA, Cheeseman JR, Zakrzewski VG, Montgomery JA, Stratmann RE, Burant JC, Dapprich S, Millam JM, Daniels AD, Kudin KN, Strain MC, Farkas O, Tomasi J, Barone V, Cossi M, Cammi R, Mennucci B, Pomelli C, Adamo C, Clifford S, Ochterski J, Petersson GA, Ayala PY, Cui Q, Morokuma K, Malick DK, Rabuck AD, Aghavachari K, Foresman JB, Cioslowski J, Ortiz JV, Stefanov BB, Liu G, Liashenko A, Piskorz P, Komaromi I, Gomperts R, Martin RL, Fox DJ, Keith T, Al-Laham MA, Peng CY, Nanayakkara A, Gonzalez C, Challacombe M, Gill PMW, Johnson BG, Chen W, Wong MW, Andres JL, Head-Gordon M, Replogle ES, Pople JA (2002) Gaussian, vol 98. Gaussian, Inc., Pittsburgh
65. Thanikachalam V, Jayabharathi J, Arunpandiyan A, Ramanathan P (2014) Photophysical properties of the intramolecular excited charge–transfer states of π-expanded styryl phenanthrimidazoles – Effect of solvent polarity, RSC advances 4:6790–6806
66. Jayabharathi J, Thanikachalam V, Srinivasan N, Jayamoorthy K, Venkatesh Perumal M (2011) An intramolecular charge transfer fluorescent probe: synthesis, structure and selective fluorescent sensing of Cu^{+2}. J Fluoresc 21:1813–1823
67. Jayabharathi J, Thanikachalam V, Jayamoorthy K, Venkatesh Perumal M (2011) A physiochemical study of excited state intramolecular proton transfer process: luminescent chemosensor by spectroscopic investigation supported by *ab initio* calculations. Spectrochim Acta A 79:6–16
68. Jayabharathi J, Thanikachalam V, Venkatesh Perumal M, Srinivasan N (2011) A physiochemical study of azo dyes: DFT based ESIPT process. Spectrochim Acta A 83:200–206
69. Jayabharathi J, Thanikachalam V, Saravanan K, Venkatesh Perumal M (2011) Spectrofluorometric studies on the binding interaction of bioactive imidazole with bovine serum albumin: a DFT based ESIPT process. Spectrochim Acta A 79:1240–1246
70. Yu W-S, Cheng C-C, Cheng Y-M, Wu P-C, Song Y-H, Chi Y, Chou P-T (2003) J Am Chem Soc 125:10800–10801
71. Hobza P, Havlas Z (2000) Blue-shifting hydrogen bonds. Chem Rev 100:4253–4264
72. Chakraborty A, De R, Guchhait N (2006) Dissection of methyl internal rotational barrier in thioacetone. Chem Phys Lett 432:616–622
73. Maheshwary S, Chowdhury A, Sathyamurthy N, Mishra H, Tripathi HB, Panda M, Chandrasekhar J (1999) J Phys Chem A 103:6257–6262
74. Bigelow RW, Johnson GE (1977) J Phys Chem 66:4861–4871
75. Gudipati MS, Daverkausen J, Maus M, Hohlneicher G (1944) Higher electronically excited states of phenanthrene, carbazole and fluorene. Chem Phys 186:289–301
76. Chiba K, Aihara JI, Araya K, Matsunaga Y (1980) Bull Chem Soc Jpn 53:1703
77. Goswami S, Sen D, Das NK, Fun HK, Quah CK (2011) A new rhodamine based colorimetric 'off-on' fluorescence sensor selective for Pd2+ along with the first bound X-ray crystal structure. Chem Commun 47:9101–9103
78. Goswami P, Das DK (2012) New highly sensitive and selective fluorescent cadmium sensor. J Fluoresc 22:391–395
79. Sherk-Bahae M, Said AA, Wei TH, Hagan DJ, Van Stryland EW (1990) Sensitive measurement of optical nonlinearities using a single beam. IEEE J Quantum Electron 26:760–769
80. Said AA, Sherk-Bahae M, Hagan DJ, Wei TH, Wang J, Young J, Van Stryland EW (1992) Determination of bound-electronic and free-carrier nonlinearities in ZnSe, GaAs, CdTe, and ZnTe. J Opt Soc Am B 9:405–414